Advanced Journal for STEM Education, Vol. 1 No. 2 (2023)
https://doi.org/10.31098/ajosed.v1i2.1854

Check for updates

Research Paper

Simply Calculating Dye Adsorption in ZIF-8 Based on External Surface Area

Ba Luan Tran[1], Thi Hong Nga Tran
[1]Can Tho University of Technology, Vietnam

Received: Sept 28, 2023	Revised: Oct 16, 2023	Accepted: Nov 5, 2023	Online: Nov 30, 2023

Abstract

We use two kinds of ZIF-8 crystals in the different external surface areas to examine the adsorption performance for three kinds of dye (Rhodamine B -RB, methyl orange -MO, and methylene blue -MB). A t-plot method was used to determine the external surface area for these samples. By establishing the trend lines from dye adsorption capacities versus external surface area, it was suggested that the RB and MO covered only on external surface area, while MB adsorbed both inside the structure of ZIF-8 and on the outer surface. Moreover, the detailed adsorption of three dyes on the sorbent can be simulated by this method. As a result, the RB and MO occupied 4.7 and 7.9 nm2 of the external surface for each molecule, respectively while that of MB included both inside the ZIF-8 structure, at a loading of 0.11 molecule per unit cell, and on the external surface with 2.3 nm2/molecule).

Keywords *t-plot method, external surface area, external and internal adsorption*

INTRODUCTION

As known, some dyes such as RB, MO, and MB are often studied to examine the capacity of adsorbent (Adeyemo et al., 2017; Feng et al., 2016; G. Li et al., 2019; T. T. Li et al., 2018). However, the adsorptive behavior inside or outer of these agents on MOFs materials seems not clear because the size of dyes is larger than that of MOFs. Regarding to this problem, Li has reported an important result about the adsorption of the dyes on ZIF-8 (G. Li et al., 2019; Y. Li et al., 2016a). The adsorption value of RB (21.4 mg/g) and MO (9.2 mg/g) may occur on the external surface area (Haque et al., 2010; He et al., 2014). In contrast, this is not correct for MB and needs more information to identify the external surface area in this case (Haque et al., 2011; Shi et al., 2016). Thus, since RB and MO only absorb on the external surface of the ZIF-8 crystals, this method can be used to estimate the external surface again when knowing the RB and MO adsorption capacity. In general, this work demonstrated that dye adsorption inside the structure and on the external surface area was directly stimulated by the graph of adsorption capacity versus the external surface area of the ZIF-8 particles. The method also can be extended using an easy way to estimate the external surface area of ZIF-8 based on a simple dye adsorption process for RB and MO.

EXPERIMENTAL SECTION

In a typical synthesis, the sample the US1 (smaller external surface area) was prepared for mixing Zn:Hmim: NH3:H2O ratio of 1:2:32:372 (Pan et al., 2011). The mixture was sonicated for 10 min to produce the US1 which was collected by centrifugation and washed with deionized water, and ethanol (95 vol %) until the pH level of the last supernatant reached 7 and final overnight drying at 90oC. On the other hand, the US2 (larger external surface area) sample was synthesized by adding

Corresponding author's email: abdullahi.ismailabubakar@ssu.edu.ng

surfactant (Pluronic® P-127, Sigma-Aldrich) in the same as described above. A mixture having a Zn:Hmim: NH3:P-127:H2O ratio of 1:2:8:0.01:316 was formulated and allowed to react for ten minutes in the ultrasonic bath. The resulting powders were collected, washed, and dried as described above, followed by another 3h at 140oC. Herein, two samples (US1 and US2) are similar procedures of synthesis but US2 was added co-polymer P-127 where can find a higher value of external surface area.

Dye adsorption experiments

The concentration range of the aqueous dye solution employed for MO and RB was 10-50 mg/L, while that for MB was 10-100 mg/L. In a typical test, 10 mg of ZIF-8 was added to 10 mL of dye solution in a vial with a cap. The capped vial was stirred at room temperature (2h for MO and RB, 48h for MB) until equilibrium was reached [1]. Afterward, the clear supernatant was collected by syringe filter (PTFE, hydrophobic, 0.22µm), and its absorbance was measured by a UV-vis spectrometer (SCINCO S-3100).

FINDINGS AND DISCUSSION

Calculated external surface area

Nitrogen isotherm measurements were conducted by using Micromeritics ASAP 2010, after vacuum activation at 120oC for 4h to determine the porosity and surface properties. The N2 adsorption isotherm (Figure 1-1) of US1 is confirmed on Type I of microporous contribution, while that of US2 exhibits a narrow hysteresis loop at high relative pressure, indicating the existence of inter-particle meso- and macropores (Peng et al., 2021). From these adsorption isotherms, the texture properties of the two ZIF-8 samples were calculated and listed in Table 1. Especially, t-plot method was applied for US1 and US2, using the Harkins-Jura equation from N2 sorption data in a thickness range of 3 to 8 Å (shown in Figure 1-2), for calculating the micro/mesopore volume and the external surface area. The intercept from the t-plot lines gives microporous volume while the slope is relative to the external surface area. In addition, the intercept of the dashed line with the y-axis provides an estimate for the total porous volume. These volumes are converted to the surface area under the setting program beforehand. Therefore, the external surface area (related to non-microporous) was calculated by extraction between the total surface and the microporous surface area. Moreover, the slope of the t-plot line US2 was 6.2 times higher than that of US1, matching the increased value of external surface area from US2 compared to US1 shown in Table 1. Clearly, under the procedure above, two samples of ZIF-8 with different external surface areas with a pure phase of two samples (shown in adding information) have been successfully obtained.

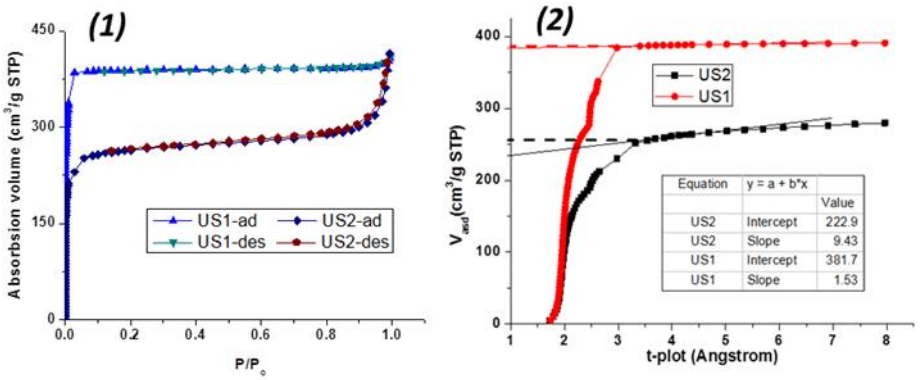

Figure 1. N_2 adsorption-desorption isotherm and t-plots line of US1 and US2

Table 1. Recipe and texture properties of US1 and US2

	Zn: NH_3:P-127:H_2O Ratio	Duration (min)	S_{BET} (m^2/g)	Surface area Micro (m^2/g)	External surface area (m^2/g)	Volume Micro/mesopore (cm^3/g)	Particle size (nm)
US1	1:32:0:372	10	1285	1261	24	0.59/0.02	2.0 x 10^3
US2	1:8:0.01:316	10	891	745	146	0.34/0.15	50-100

Experimental adsorption capacity

To calculate the amount of dye adsorbed inside the ZIF-8 structure and outer surface, trend lines of dye adsorption capacities versus external surface area were set up using experimental results for US1 and US2, as shown in Figure 2. The capacity of the internal structure is estimated by the intercept while the slope supplies that on the external surface area. The fact that RB and MO lines pass through the origin is evident that the RB and MO dye were only uptaken by the presence of external surface area. Therefore, the RB and MO covered the external surface area and had no entry to the ZIF-8 structure. In contrast, the MB line informs that this dye adsorbed both inside the ZIF-8 structure (showed by a considerable intercept) and on the external surface area. The detailed calculation of adsorption capacity adsorbs on the sorbent using related data from this method is performed below and listed in Table 2.

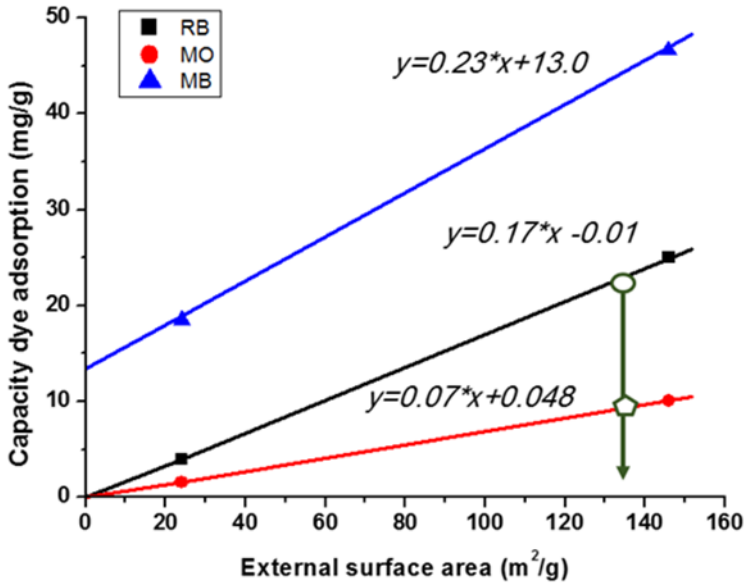

Figure 2. Adsorption capacities of three dyes versus external surface area. Related linear fit models are shown for each case

From Figure 2, the number of dye molecules adsorbed on the external surface area, Nex (molecules/nm2) was obtained by the following equation:

$$N_{ex} = 10\text{^}18/(q\__{ex}/(1000*M)*N)$$

Where $_{sex}$ is a value from the slopes of trend lines of dye adsorption capacities versus external surface area (mg/m^2), N is Avogadro's number (6.023 x1023 molecules.mol^{-1}), and M is the molecular weight of dye (g/mol). The calculated results are then converted to the number of molecules per unit surface area. Moreover, the coverage adsorption for three dyes on the external surface area was detailed in supporting information.

On the other hand, the number of dye molecules adsorbed inside each unit cell of ZIF-8 (Nin) was calculated by this equation:

$N_{in} = (q\__i/((M*1000)))/(1/〖MW〗\_(ZIF\text{-}8))*12$

Where q_i (mg/g) is the value of intercept given by trend lines of dye adsorption capacities versus external surface area (Figure 2), MW_{ZIF-8} is the molecular weight of ZIF-8 (formula of Zn(MeIM)2, 277.6 g.mol-1), and every ZIF-8 unit cell consists of 12 zinc atoms[4]. Therefore, only MB is considered to adsorb inside the structure in a large amount (13.0 mg/g), which can be calculated to be 0.11 molecules per unit cell.

Table 2. Adsorption capacity of dyes in US1 and US2

[a]Dye molecule weight (g/mol)	Sample	Adsorption capacity (mg/g)	Intercept (mg/g)	N_{in}, internal adsorption (#/unit cell)	Slop (mg/m^2)	N_{ex}, external adsorption ($\#/nm^2$)
RB: 479	US1	4.1	-0.01	$-6x10^{-5}$	0.17	0.21
	US2	25.0				
MO: 327	US1	1.7	0.048	$4x10^{-4}$	0.07	0.13
	US2	10.1				
MB: 320	US1	18.5	13.0	0.11	0.23	0.43
	US2	46.6				

Adding Information

Characterizations of two ZIF-8 crystals

Two samples were characterized by some physical techniques to confirm the pure phase and morphologies of ZIF-8 such as Powder X-ray diffraction (PXRD) patterns and field emission scanning electron microscopy (FE-SEM). The XRD were recorded between 5° and 40° using a Cu Kα radiation (40 mA and 40 kV) source on a D8 Advance Bruker powder diffractometer at a scan rate of 5°/min and a step size of 0.03° and the SEM were observed on a JEOL JSM-7600F operated at 10kV. Both US1 and US2 exhibit a pure phase ZIF-8 as verified by comparing the XRD peaks (Figure 3-1) to the literature (Butova et al., 2016; Lee et al., 2015; Peng et al., 2021; Seoane et al., 2012; Zhou et al., 2017). From the SEM images, the shape of US1 crystals is truncated cubic with a uniform particle size of ~2.0 μm, while US2 obtained crystals with a size in the range of 50-100 nm as shown in Figure 3-2 and Figure 3-3, respectively(Fan et al., 2014; Xing et al., 2014). The nanocrystal one is expecting a larger external surface which can enhance dye adsorption compared to microcrystal samples (Y. Li et al., 2016b; Tanaka et al., 2013).

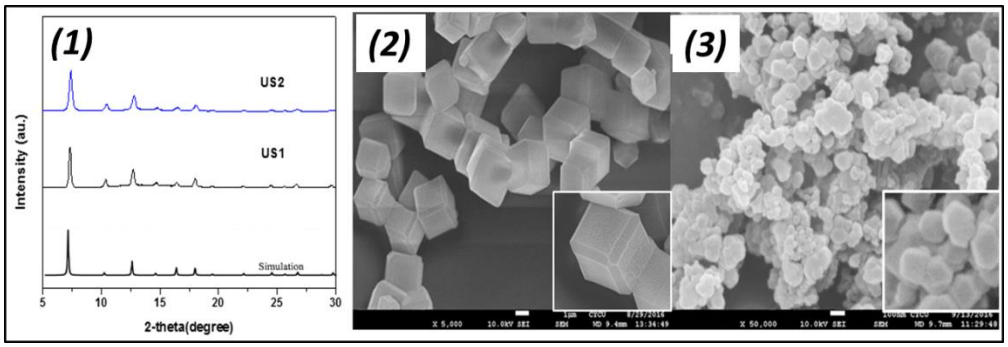

Figure 3. (1) XRD patterns, SEM images of (2) US1 and (3) US2

Calculation of the coverage adsorption on external surface area

The coverage of dye adsorption in the external surface area (C) is calculated by this equation:

$$C = N_{ex} \times A_{dye}$$

Where N_{ex} is the amount of dye molecules adsorbed on the external surface area, ($\#/nm^2$) and A_{dye} is the maximum area of dye molecules was calculated by using the longest two dimensions of the molecular structure(Han et al., 2017). As results from Table 2, the coverage of three dyes on the external surface area increased in order MO < MB < RB.

Table 2. Calculation of the coverage of dye adsorption

Dye	Dye molecule size (nm)	A_{dye}, Molecule Area (nm^2)	C, Coverage (%)
RB	1.59 x 1.18 x 0.56	1.88	39.5
MO	1.31 x 0.55 x 0.18	0.72	9.4
MB	1.39 x 0.50 x 0.43	0.69	29.7

CONCLUSIONS

In conclusion, we set up a new simple method to calculate three kinds of Dye which adsorption to ZIF-8. It was found that the size of dye molecules is strongly affected by the adsorbed process. Based on the flexible structure of ZIF-8, the number of dye molecules should be calculated in detail outside the structure of the adsorbent through the liner method. It is necessary to study more for dye both adsorbed outer and inside the structure of ZIF-8. This work aims to open new ways to deeply understand the adsorption studies under the effect of particle sizes and external surface area.

REFERENCES

Adeyemo, A. A., Adeoye, I. O., & Bello, O. S. (2017). Adsorption of dyes using different types of clay: a review. *Applied Water Science*. https://doi.org/10.1007/s13201-015-0322-y

Butova, V. V., Budnik, A. P., Bulanova, E. A., & Soldatov, A. V. (2016). New microwave-assisted synthesis of ZIF-8. *Mendeleev Communications*, *26*(1), 43–44. https://doi.org/10.1016/j.mencom.2016.01.017

Fan, X., Wang, W., Li, W., Zhou, J., Wang, B., Zheng, J., & Li, X. (2014). Highly Porous ZIF-8 Nanocrystals Prepared by a Surfactant Mediated Method in Aqueous Solution with Enhanced Adsorption Kinetics. *ACS Applied Materials & Interfaces*, *6*(17), 14994–14999. https://doi.org/10.1021/am5028346

Feng, Y., Li, Y., Xu, M., Liu, S., & Yao, J. (2016). Fast adsorption of methyl blue on zeolitic imidazolate framework-8 and its adsorption mechanism. *RSC Advances*, *6*(111), 109608–109612. https://doi.org/10.1039/C6RA23870J

Han, Y., Liu, M., Li, K., Sun, Q., Zhang, W., Song, C., Zhang, G., Conrad Zhang, Z., & Guo, X. (2017). In situ synthesis of titanium doped hybrid metal-organic framework UiO-66 with enhanced adsorption capacity for organic dyes. *Inorganic Chemistry Frontiers*, *4*(11), 1870–1880. https://doi.org/10.1039/C7QI00437K

Haque, E., Jun, J. W., & Jhung, S. H. (2011). Adsorptive removal of methyl orange and methylene blue from aqueous solution with a metal-organic framework material, iron terephthalate (MOF-235). *Journal of Hazardous Materials*, *185*(1), 507–511. https://doi.org/10.1016/j.jhazmat.2010.09.035

Haque, E., Lee, J. E., Jang, I. T., Hwang, Y. K., Chang, J.-S., Jegal, J., & Jhung, S. H. (2010). Adsorptive removal of methyl orange from aqueous solution with metal-organic frameworks, porous chromium-benzenedicarboxylates. *Journal of Hazardous Materials*, *181*(1–3), 535–542. https://doi.org/10.1016/j.jhazmat.2010.05.047

He, M., Yao, J., Liu, Q., Wang, K., Chen, F., & Wang, H. (2014). Facile synthesis of zeolitic imidazolate framework-8 from a concentrated aqueous solution. *Microporous and Mesoporous Materials*, *184*, 55–60. https://doi.org/10.1016/j.micromeso.2013.10.003

Lee, Y. R., Jang, M. S., Cho, H. Y., Kwon, H. J., Kim, S., & Ahn, W. S. (2015). ZIF-8: A comparison of synthesis methods. *Chemical Engineering Journal*, *271*, 276–280. https://doi.org/10.1016/j.cej.2015.02.094

Li, G., Xia, L., Dong, J., Chen, Y., & Li, Y. (2019). Metal-organic frameworks. In *Solid-Phase Extraction* (pp. 285–309). Elsevier. https://doi.org/10.1016/B978-0-12-816906-3.00010-8

Li, T. T., Liu, Y. M., Wang, T., Wu, Y. L., He, Y. L., Yang, R., & Zheng, S. R. (2018). Regulation of the surface area and surface charge property of MOFs by multivariate strategy: Synthesis,

characterization, selective dye adsorption and separation. *Microporous and Mesoporous Materials*. https://doi.org/10.1016/j.micromeso.2018.06.023

Li, Y., Zhou, K., He, M., & Yao, J. (2016a). Synthesis of ZIF-8 and ZIF-67 using mixed-base and their dye adsorption. *Microporous and Mesoporous Materials*, *234*, 287–292. https://doi.org/http://dx.doi.org/10.1016/j.micromeso.2016.07.039

Li, Y., Zhou, K., He, M., & Yao, J. (2016b). Synthesis of ZIF-8 and ZIF-67 using mixed-base and their dye adsorption. *Microporous and Mesoporous Materials*, *234*, 287–292. https://doi.org/http://dx.doi.org/10.1016/j.micromeso.2016.07.039

Pan, Y., Liu, Y., Zeng, G., Zhao, L., & Lai, Z. (2011). Rapid synthesis of zeolitic imidazolate framework-8 (ZIF-8) nanocrystals in an aqueous system. *Chemical Communications*, *47*(7), 2071. https://doi.org/10.1039/c0cc05002d

Peng, J., Zhang, Z., Hu, C., Wang, Z., Kang, Y., Chen, W., & Ao, T. (2021). Hierarchically porous ZIF-8 for tetracycline hydrochloride elimination. *Journal of Sol-Gel Science and Technology*, *99*(2), 339–353. https://doi.org/10.1007/s10971-021-05576-0

Seoane, B., Zamaro, J. M., Tellez, C., & Coronas, J. (2012). Sonocrystallization of zeolitic imidazolate frameworks (ZIF-7, ZIF-8, ZIF-11 and ZIF-20). *CrystEngComm*, *14*(9), 3103–3107. https://doi.org/10.1039/C2CE06382D

Shi, L., Hu, L., Zheng, J., Zhang, M., & Xu, J. (2016). Adsorptive Removal of Methylene Blue from Aqueous Solution using a Ni-Metal Organic Framework Material. *Journal of Dispersion Science and Technology*, *37*(8), 1226–1231. https://doi.org/10.1080/01932691.2015.1050731

Tanaka, S., Kida, K., Nagaoka, T., Ota, T., & Miyake, Y. (2013). Mechanochemical dry conversion of zinc oxide to zeolitic imidazolate framework. *Chemical Communications*, *49*(72), 7884–7886. https://doi.org/10.1039/C3CC43028F

Xing, T., Lou, Y., Bao, Q., & Chen, J. (2014). Surfactant-assisted synthesis of ZIF-8 nanocrystals in aqueous solution via microwave irradiation. *CrystEngComm*, *16*(38), 8994–9000. https://doi.org/10.1039/C4CE00947A

Zhou, K., Mousavi, B., Luo, Z., Phatanasri, S., Chaemchuen, S., & Verpoort, F. (2017). Characterization and properties of Zn/Co zeolitic imidazolate frameworks vs. ZIF-8 and ZIF-67. *Journal of Materials Chemistry A*, *5*(3), 952–957. https://doi.org/10.1039/C6TA07860E